AGU PUBLICATIONS

Geophysical Research Letters

RESEARCH LETTER
10.1002/2016GL071082

Key Points:
- A new method of estimating mesopause temperatures using meteor radar observations is proposed
- The height distribution of meteor trails is primarily determined using the background atmospheric pressure level
- The width of the meteor height distribution presents a consistent linear relationship with the temperature at the meteor peak height

Correspondence to:
J.-H. Kim,
jhkim@kopri.re.kr

Citation:
Lee, C., J.-H. Kim, G. Jee, W. Lee, I.-S. Song, and Y. H. Kim (2016), New method of estimating temperatures near the mesopause region using meteor radar observations, *Geophys. Res. Lett.*, *43*, 10,580–10,585, doi:10.1002/2016GL071082.

Received 27 JUN 2016
Accepted 10 OCT 2016
Accepted article online 12 OCT 2016
Published online 27 OCT 2016

New method of estimating temperatures near the mesopause region using meteor radar observations

Changsup Lee[1], Jeong-Han Kim[1], Geonhwa Jee[1], Wonseok Lee[2], In-Sun Song[1], and Yong Ha Kim[2]

[1]Korea Polar Research Institute, Incheon, South Korea, [2]Department of Astronomy, Space Science and Geology, Chungnam National University, Daejeon, South Korea

Abstract We present a novel method of estimating temperatures near the mesopause region using meteor radar observations. The method utilizes the linear relationship between the full width at half maximum (FWHM) of the meteor height distribution and the temperature at the meteor peak height. Once the proportionality constant of the linear relationship is determined from independent temperature measurements performed over a specific period of time by the Microwave Limb Sounder (MLS) instrument on board the Aura satellite, the temperature can be estimated continuously according to the measurements of the FWHM alone without additional information. The temperatures estimated from the FWHM are consistent with the MLS temperatures throughout the study period within a margin of 3.0%. Although previous methods are based on temperature gradient or pressure assumptions, the new method does not require such assumptions, which allows us to estimate the temperature at approximately 90 km with better precision.

1. Introduction

Although the mesosphere and lower thermosphere (MLT) region is difficult to access, the neutral temperature of the MLT is an essential parameter for understanding the physical processes underlying the region's dynamical variations and their long-term trends in response to climate change. Recent developments in meteor radar have increased the usefulness of this technology for investigations of the MLT region, and meteor radar is particularly effective for inferring the neutral temperature near the mesopause region because it is capable of operating day and night all year round, regardless of the weather conditions. The optical instruments that observe airglow in the mesosphere provide information on mesospheric temperatures. However, these instruments are intrinsically limited because they can only operate during moonless clear nights [*Won et al.*, 2003; *Cho et al.*, 2010]. Hence, a number of studies have been performed on meteor radar observations, which do not present such a limitation, and reports indicate that meteor radar can successfully and continuously monitor mesospheric temperatures [*Chilson et al.*, 1996; *Hocking et al.*, 1997; *Stober et al.*, 2008; *Hall et al.*, 2012; *Kim et al.*, 2012].

To estimate the mesospheric temperature from meteor radar observations, most previous studies utilized the linear relationship between the diffusion coefficient obtained from the meteor decay time and $T/P^{1/2}$, where T and P are atmospheric temperature and pressure, respectively [*Hocking et al.*, 2004; *Holdsworth et al.*, 2006]. To overcome the requirement of a priori atmospheric pressure knowledge to perform temperature estimations, *Hocking* [1999] proposed the following relationship:

$$T = S\left(\frac{mg}{k} + 2\frac{\mathrm{d}t}{\mathrm{d}z}\right) log_{10}e, \tag{1}$$

where S is the slope of the log inverse decay time versus the height, m is the mass of a typical atmospheric molecule, g is the gravitational acceleration near the meteor height, k is the Boltzmann constant, and $\mathrm{d}T/\mathrm{d}z$ is the temperature gradient. From equation (1), the temperature at the meteor peak height can be estimated once the meteor decay time profiles are obtained from meteor radar observations. Several observational studies have been conducted to validate or improve this method via comparisons between temperatures derived from pressure models and airglow observations from the ground and satellites [*Hocking et al.*, 2001; *Singer et al.*, 2004; *Vineeth et al.*, 2005; *Hocking et al.*, 2007; *Kumar*, 2007; *Dyrland et al.*, 2010; *Kim et al.*, 2012; *Meek et al.*, 2013].

Although the temperature estimated from this method is generally consistent with other independent measurements, the method requires the following a priori information: (1) the temperature gradient model based on other independent temperature observations and (2) the slope of the height profiles of the log inverse decay time [*Kim et al*., 2012]. However, a consistent method of determining the slope is not available because each study has applied different criteria for determining this parameter, which increases the difficultly of directly comparing or validating the results estimated from various locations. In this study, we propose a new method for estimating mesospheric temperatures from meteor radar observations without a priori information on the temperature gradient and slope. We will compare the results from the new method with those from the temperature gradient method and the temperature measurements of the Microwave Limb Sounder (MLS) on board the Aura satellite.

2. Observations

2.1. Meteor Radar at King Sejong Station

The meteor radar is designed to observe the mesosphere and lower thermosphere (MLT) region at an altitude of 70 to 110 km by detecting the backscattered signals from the ionized meteor trails. The meteor radar at King Sejong Station (KSS) in Antarctica (62.22°S, 58.78°W) has been operated by the Korea Polar Research Institute in cooperation with Chungnam National University, Korea, since March 2007. The KSS meteor radar is configured at a frequency of 33.2 MHz, which is an optimized condition for a maximum meteor detection rate. The transmitter has a peak power of 12 kW and a duty cycle of 8.4% for coded Gaussian-shaped pulses at a pulse repetition rate of 440 Hz. The typical meteor detection rate of the KSS meteor radar is 15,000–40,000 unambiguous underdense meteors per day, which shows clear seasonal variation, with a maximum in summer and a minimum in winter [*Kim et al*., 2010; *Lee et al*., 2013; *Eswaraiah et al*., 2016]. The large detection rate of the KSS radar allows us to extend the height range of the reliable meteor information from the peak meteor detection height down to an altitude of approximately 75 km without excessive uncertainty. Radar data from 2012 to 2015, which represent a period with sufficient recordings of meteors, even in winter, are used because the observed meteor distribution statistics critically depend on the meteor detection rate.

2.2. Aura/MLS Data

The neutral temperature and geopotential height (GPH) data at meteor heights were obtained from Aura satellite observations near KSS. The Aura satellite is in a Sun-synchronous polar orbit at an altitude of 705 km with an inclination of 98.2°. The MLS instrument on board the Aura satellite measures microwave emissions across five bands ranging from 118 GHz to 2.5 THz to derive the temperatures and constituent volume mixing ratios on the fixed pressure surfaces from the troposphere to the mesosphere. The MLS temperature and GPH are primarily retrieved from a band close to the O_2 spectral lines at 118 GHz on a fixed vertical pressure grid from 261 hPa to 0.001 hPa. The horizontal resolution of the temperature is 165 km along the orbital track and 21 km across the track [*Schwartz et al*., 2008]. In this study, we used the MLS data from both the ascending and descending nodes within a distance of 400 km centered on the location of KSS to directly compare the satellite data with the meteor radar observations over the entire period from 2012 to 2015. All of the MLS GPHs were converted to geometric heights as described in *Younger et al*. [2014], and the Earth's radius at the latitude of the observations was based on the WGS84 ellipsoid model.

3. Height Distribution of Meteor Echoes

Most underdense meteors ablate in the altitude region from 70 to 110 km because of collisions with atmospheric molecules. The resulting meteor plasma trails provide essential information on the background atmosphere, including the neutral wind, temperature [*Kim et al*., 2012], and density [*Younger et al*., 2015]. The meteor radar detects echoes backscattered from the meteor trails aligned perpendicular to the line of sight. The detected meteors are mostly concentrated at an altitude of approximately 90 km, and the meteor peak height (MPH) is sensitively dependent on the background atmospheric density [*McKinley*, 1961]. The height distribution of the meteor echoes, however, primarily depends on the atmospheric density gradient (i.e., the atmospheric scale height) and mass distribution of the incident meteors [*Kaiser*, 1954].

Figure 1 shows the meteor height distribution observed by the KSS meteor radar on a day in 2013 for which the maximum number of meteor echoes was recorded. Because a Gaussian function best fits the observed

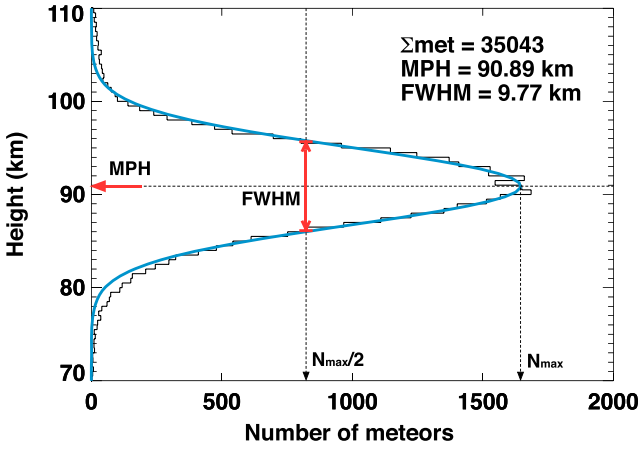

Figure 1. Histogram of the height distribution of a total of 35,043 meteors recorded on 1 January 2013 using a 500 m height bin. The fitted Gaussian curve for the estimation of MPH and FWHM is depicted as a blue solid line.

meteor height distribution, at least near the peak, we fit the distribution with a Gaussian curve by adjusting the MPH and the full width at half maximum (FWHM) as presented in Figure 1.

The daily values of the MPH and FWHM calculated from meteor radar observations in 2014 and the heights of the constant atmospheric pressure surfaces from MLS observations within a region of 400 km centered on KSS are presented in Figure 2. The MPH was highly correlated with the height of the atmospheric pressure at $\log_{10} P = -3.11$. The heights of the constant pressure surfaces varied with the seasons because of the corresponding atmospheric expansions and contractions. The FWHMs (red) around the MPHs (blue diamond) are also displayed. The height intervals of the two neutral pressure surfaces above and below the MPH are well followed by the FWHM. These results show that the height distribution of the meteor echoes is mainly affected by the background atmospheric pressure, which is a function of density and temperature.

The high correlation between the FWHM and the background atmospheric pressure shown in Figure 2 can be described by a hydrostatic equation:

$$\frac{\partial \ln P}{\partial z} = -\frac{g}{RT}, \tag{2}$$

where g and R are the gravitational acceleration and gas constant, respectively. These two parameters can be considered constant within a small-altitude range around the MPH in the well-mixed atmosphere below 100 km [*Andrews et al.*, 1987]. The FWHM closely follows the two pressure surfaces of $P_1(z_1)$ and $P_2(z_2)$ as indicated by the two thick lines enveloping the FWHM in Figure 2. This result may indicate that the FWHM represented by the height difference is directly proportional to the temperature within the atmospheric layers between the two pressure surfaces at z_1 and z_2:

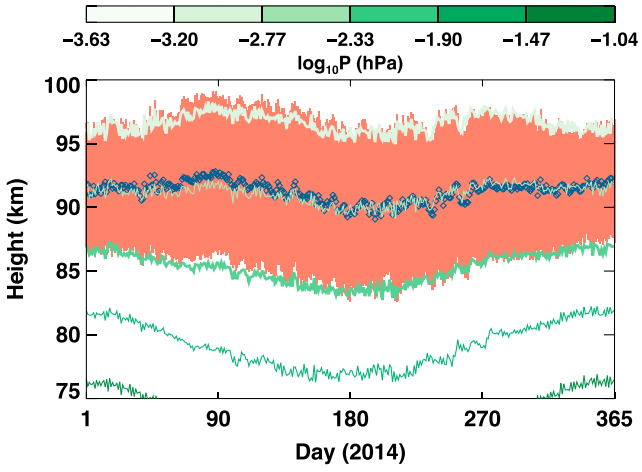

Figure 2. Heights of the constant pressure surfaces of the neutral atmosphere from the Aura MLS (contours) and meteor peak detection heights (blue diamond) with full width at half maximum (FWHM) of the meteor distribution (red shaded area) from the meteor radar observations at King Sejong Station, Antarctica performed throughout 2014.

$$\mathrm{FWHM} = \frac{R}{g} \ln\left(\frac{P_1}{P_2}\right) \langle T \rangle, \tag{3}$$

where FWHM = $z_2 - z_1$ and p_1 and p_2 are constant. Note that this relationship can simply be derived from equation (2). The layer mean temperature $\langle T \rangle$ between the two constant pressure surfaces of $P_1(z_1)$ and $P_2(z_2)$ is defined as follows:

$$\langle T \rangle = \int_{P_1}^{P_2} T \, d\ln P \Big/ \int_{P_1}^{P_2} d\ln P. \tag{4}$$

Holdsworth et al. [2006] found that the width of the meteor height distribution is linearly correlated with the temperatures derived from meteor decay time profiles. Here we present the scatterplot of the daily values throughout 2013 of the FWHM observed by the KSS meteor radar versus the Aura/MLS temperature

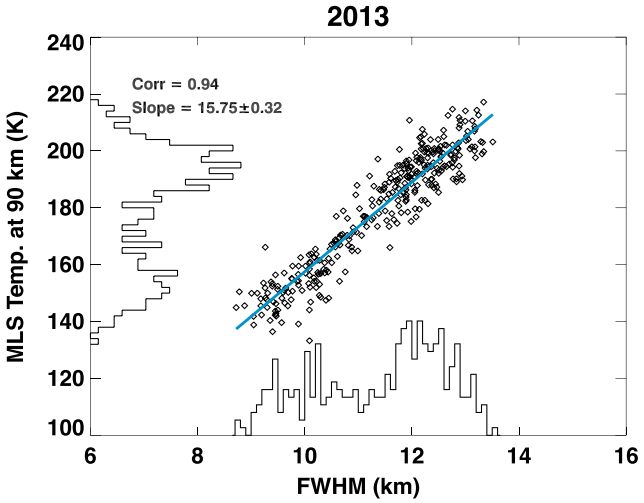

Figure 3. Scatterplot of the daily FWHM of the meteor height distribution versus the average value of the MLS temperatures at 90 km at King Sejong Station in 2013. The blue solid line depicts the linear regression. The histograms of the MLS temperature and FWHM data are also presented to show the overall quantity of the data of the scatter plot.

at a height of 90 km (Figure 3). Figure 3 shows that the FWHM has a clear linear relationship with temperature and presents a well-defined slope with a correlation coefficient of 0.94. The slope of 15.75 in Figure 3 represents the proportionality constant between the FWHM and temperature. Note that the proportionality constant between the FWHM and the mesopause temperature does not appear to change over time, which is shown in Table 1. This nearly invariable proportionality constant allows us to estimate the temperature at the meteor peak altitude (~90 km) by using only the FWHM data observed by the meteor radar. *Kozlovsky et al*. [2016] indicated that the temperature estimation from meteor decay times can be severely affected by meteor showers because of the peculiar distribution of the meteor decay time within the meteor showers. However, we found that the effects of meteor showers on the linear relationship between the FWHM and the temperature at 90 km are negligible. Therefore, all of the observed meteor data are used in this study.

Using the proportionality constant of 15.71 averaged over 4 years from 2012 to 2015, we calculated the temperature at 90 km from the measured FWHM for 2014 and 2015 under the assumption that the characteristics of the meteor influxes (i.e., mass and velocity distributions of the meteors) do not change significantly during the meteor radar observation periods. Figure 4 shows the estimated daily temperatures (T_{FWHM}) at 90 km from the FWHM of the height distribution of the meteor echoes from 2014 to 2015. Figure 4 also shows the temperatures (T_{diff}) estimated from the previous method that utilized the slopes of the meteor decay time profiles in a temperature gradient model. The detailed temperature estimation procedure in the previous method is described in *Kim et al*. [2012]. The observed temperatures (T_{MLS}) from Aura/MLS instrument are also presented for the evaluation of the results from the two temperature estimation methods. The vertical resolution of the MLS temperature measurement near 90 km is 13 km, and it has a precision of 3 K. Cubic spline interpolation was applied to the MLS raw temperature data, which generated temperatures with even height intervals of 2 km, to obtain the MLS temperature near the meteor peak height. The comparison in Figure 4 shows that the temperatures estimated from the FWHM well represent the annual variations as well as the overall day-to-day variability in the mesospheric temperatures. The values are consistent with the MLS temperatures (on average, 2.86 ± 2.42% difference). The temperatures derived from the meteor decay times, however, show larger day-to-day variability and severely overestimate the temperature in summer (on average, 5.63 ± 5.37% difference).

Table 1. Slope Values Exhibiting a Linear Relationship Between the MLS Temperature at 90 km and the FWHM From the Meteor Radar at KSS From 2012 to 2015

Year	Slope	Correlation Coefficient
2012	15.607 ± 0.373	0.922
2013	15.752 ± 0.321	0.940
2014	15.724 ± 0.332	0.925
2015	15.754 ± 0.334	0.924
Mean	15.709 ± 0.340	0.927

4. Summary and Conclusions

In this study, we presented a new method for estimating the temperature near the mesopause region using the linear relationship between the width of the meteor height distribution and the vertical gradient of the background atmospheric pressure. The temperature at the meteor peak height can be estimated from observations of the width

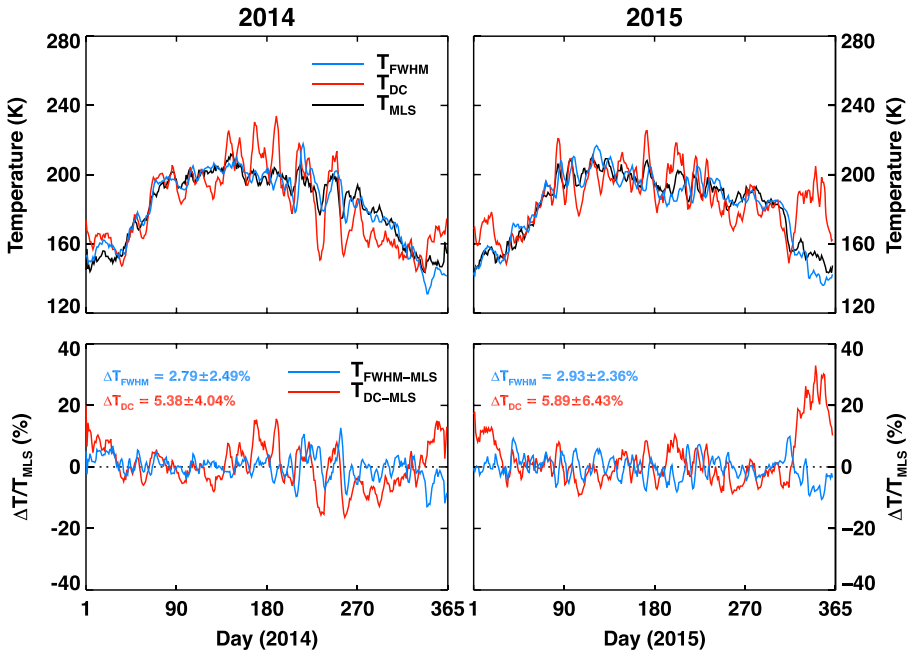

Figure 4. (top row) A comparison of the daily mean temperatures estimated using the FWHM (blue line) and meteor decay times (red line) and the temperatures recorded by the MLS (black line) in (left column) 2014 and (right column) 2015. (bottom row) The relative temperature differences between the two different temperature estimations and the MLS observations are also displayed with the corresponding standard deviations.

of the meteor height distribution because the atmospheric pressure gradient directly depends on the atmospheric temperature. Although current methods utilize the temperature dependence of the diffusion process within meteor trails, the new method uses a totally different physical characteristic of the meteor observation: the dependence of the meteor height distribution on the vertical gradient of the atmospheric pressure (i.e., atmospheric temperature). Furthermore, the proportionality constant between the width of the meteor distribution and the temperature was nearly constant at KSS throughout the entire observational period. Therefore, once the constant is determined from the independent temperature measurements (MLS temperature in this study) over a certain period of time, the temperature can continuously be estimated from the measurements of the width alone without requiring any additional information. Finally, the initial validation of the new method shows that the estimated temperatures are more consistent with satellite observations compared with the temperatures derived from previous methods.

Acknowledgments
This study was supported by the grant PE16090 from the Korea Polar Research Institute. The authors would like to thank the Aura MLS team for providing the geopotential height and temperature data. The Aura/MLS data used in this study are available from http://disc.sci.gsfc.nasa.gov/Aura/data-holdings/MLS.

References

Andrews, D. G., J. R. Holton, and C. B. Leovy (1987), *Middle Atmosphere Dynamics*, pp. 498, Academic Press, San Diego, Calif.

Chilson, P. B., P. Czechowsky, and G. Schmidt (1996), A comparison of ambipolar diffusion coefficients in meteor trains using VHF radar and UV lidar, *Geophys. Res. Lett.*, *23*, 2745–2748, doi:10.1029/96GL02577.

Cho, Y. M., M. G. Shepherd, and G. G. Shepherd (2010), Wave perturbations in the MLT at high northern latitudes in winter, observed by two SATI instruments, *Adv. Space Res.*, *45*, 45–55, doi:10.1016/j.asr.2009.08.006.

Dyrland, M. E., C. M. Hall, F. J. Mulligan, M. Tsutsumi, and F. Sigernes (2010), Improved estimates for neutral air temperatures at 90 km and 78° N using satellite and meteor radar data, *Radio Sci.*, *45*, RS4006, doi:10.1029/2009RS004344.

Eswaraiah, S., Y. H. Kim, J. Hong, J.-H. Kim, M. V. Ratnam, A. Chandran, S. V. B. Rao, and D. Riggin (2016), Mesospheric signatures observed during 2010 minor stratospheric warming at King Sejong Station (62°S, 59°W), *J. Atmos. Sol. Terr. Phys.*, *140*, 55–64, doi:10.1016/j.jastp.2016.02.007.

Hall, C. M., M. E. Dyrland, M. Tsutsume, and F. J. Mulligan (2012), Temperature trends at 90 km over Svalbard, Norway (78°N, 16°E), seen in one decade of meteor radar observations, *J. Geophys. Res.*, *117*, D08104, doi:10.1029/2011JD017028.

Hocking, W. K. (1999), Temperatures using radar-meteor decay times, *Geophys. Res. Lett.*, *26*, 3297–3300, doi:10.1029/1999GL003618.

Hocking, W. K., T. Thayaparan, and J. Jones (1997), Meteor decay times and their use in determining a diagnostic mesospheric temperature-pressure parameter: methodology and one year of data, *Geophys. Res. Lett.*, *24*, 2977–2980, doi:10.1029/97GL03048.

Hocking, W. K., T. Thayaparan, and S. J. Franke (2001), Method for statistical comparison of geophysical data by multiple instruments which have differing accuracies, *Adv. Space Res.*, *27*(6–7), 1089–1098.

Hocking, W. K., P. S. Argall, R. P. Lowe, R. J. Sica, and H. Ellinor (2007), Height dependent meteor temperatures and comparisons with lidar and OH measurements, *Can. J. Phys.*, *85*(2), 173–187.

Hocking, W., W. Singer, J. W. Bremer, N. Mitchell, P. Batista, B. Clemesha, and M. Donner (2004), Meteor radar temperatures at multiple sites derived with SKiYMET radars and compared to OH, rocket and lidar measurements, *J. Atmos. Sol. Terr. Phys.*, *66*, 585–593.

Holdsworth, D. A., R. J. Morris, D. J. Murphy, I. M. Reid, G. B. Burns, and W. J. R. French (2006), Antarctic mesospheric temperature estimation using the Davis mesosphere-stratosphere-troposphere radar, *J. Geophys. Res.*, *111*, D05108, doi:10.1029/2005JD006589.

Kaiser, T. R. (1954), Theory of the meteor heigh distribution obtained from radio-echo observations II. Sporadic meteors, *Mon. Not. R. Astron. Soc.*, *114*(1), 52–62, doi:10.1093/mnras/114.1.52.

Kim, J.-H., Y. H. Kim, C. S. Lee, and G. Jee (2010), Seasonal variation of meteor decay times observed at King Sejong Station (62.22°S, 58.78°W), Antarctica, *J. Atmos. Sol. Terr. Phys.*, *72*(11–12), 883–889, doi:10.1016/j.jastp.2010.05.003.

Kim, J.-H., Y. H. Kim, G. Jee, and C. Lee (2012), Mesospheric temperature estimation from meteor decay times of weak and strong meteor trails, *J. Atmos. Sol. Terr. Phys.*, *89*, 18–26.

Kozlovsky, A., R. Lukianova, S. Shalimov, and M. Lester (2016), Mesospheric temperature estimation from meteor decay times during Geminids meteor shower, *J. Geophys. Res. Space Physics*, *121*, 1669–1679, doi:10.1002/2015JA022222.

Kumar, K. K. (2007), Temperature profiles in the MLT region using radar-meteor trail decay times: Comparison with TIMED/SABER observations, *Geophys. Res. Lett.*, *34*, L16811, doi:10.1029/2007GL030704.

Lee, C. S., J. P. Younger, I. M. Reid, Y. H. Kim, and J. H. Kim (2013), The effect of recombination and attachment on meteor radar diffusion coefficient profiles, *J. Geophys. Res. Atmos.*, *118*, 3037–3043, doi:10.1002/jgrd.50315.

McKinley, D. W. R. (1961), *Meteor Science and Engineering*, McGraw-Hill, New York.

Meek, C. E., A. H. Manson, W. K. Hocking, and J. R. Drummond (2013), Eureka, 80°N, SKiYMET meteor radar temperatures compared with Aura MLS values, *Ann. Geophys.*, *31*, 1267–1277, doi:10.5194/angeo-31-1267-2013.

Schwartz, M. J., et al. (2008), Validation of the Aura Microwave Limb Sounder temperature and geopotential height measurements, *J. Geophys. Res.*, *113*, D15S11, doi:10.1029/2007JD008783.

Singer, W., J. Bremer, J. Weiß, W. K. Hocking, J. Höffner, M. Donner, and P. Espy (2004), Meteor radar observations at middle and Arctic latitudes Part 1: Mean temperatures, *J. Atmos. Sol. Terr. Phys.*, *66*(6–9), 607–616, doi:10.1016/j.jastp.2004.01.012.

Stober, G., C. Jacobi, K. Fröhlich, and J. Oberheide (2008), Meteor radar temperatures over Collm (51.3°N, 13°E), *Adv. Space Res.*, *42*(7), 1253–1258, doi:10.1016/j.asr.2007.10.018.

Vineeth, C., T. K. Pant, M. Antonita, G. Ramkumar, C. V. Devasia, and R. Sridharan (2005), A comparative study of daytime mesopause temperatures obtained using unique ground based optical and meteor wind radar techniques over the magnetic equator, *Geophys. Res. Lett.*, *32*, L19101, doi:10.1029/2005GL023728.

Won, Y. I., Q. Wu, Y. M. Cho, G. G. Shepherd, T. L. Killeen, P. J. Espy, Y. Kim, and B. Solheim (2003), Polar cap observations of mesospheric and lower thermospheric 4-hour waves in temperature, *Geophys. Res. Lett.*, *30*(7), 1377, doi:10.1029/2002GL016364.

Younger, J. P., C. S. Lee, I. M. Reid, R. A. Vincent, Y. H. Kim, and D. J. Murphy (2014), The effects of deionization processes on meteor radar diffusion coefficients below 90 km, *J. Geophys. Res. Atmos.*, *119*, 10,027–10,043, doi:10.1002/2014JD021787.

Younger, J. P., I. M. Reid, R. A. Vincent, and D. J. Murphy (2015), A method for estimating the height of a mesospheric density level using meteor radar, *Geophys. Res. Lett.*, *42*, 6106–6111, doi:10.1002/2015GL065066.